

Long-Term Instrumental and Reconstructed Temperature Records Contradict Anthropogenic Global Warming

Horst-Joachim Lüdecke

EIKE, European Institute for Climate and Energy,
PO.Box 11011, 07722 Jena, GERMANY
info@cfact-europe.org
moluedecke@aol.com

Supplemented version of the article published in *Energy & Environment*, Vol. 22, No. 6 (Sept. 2011)

Abstract. Monthly instrumental temperature records from 5 stations in the northern hemisphere are analyzed, each of which is local and well over 200 years in length, as well as two reconstructed long-range yearly records - from a stalagmite and from tree rings that are about 2000 years long. In the instrumental records, the steepest 100-year temperature fall happened in the 19th century and the steepest rise in the 20th century, both events being of about the same magnitude. Evaluation by the detrended fluctuation analysis (DFA) yields Hurst exponents that are in good agreement with the literature. DFA, Monte Carlo simulations, and synthetic records reveal that both 100-year events have too small probabilities to be natural fluctuations and, therefore, were caused by external trends. In contrast to this, the reconstructed records show stronger 100-year rises and falls as quite common during the last 2000 years. Consequently, their DFA evaluation reveals far greater Hurst exponents. These results contradict the hypothesis of an unusual (anthropogenic) global warming during the 20th century. The cause of the different Hurst exponents for the instrumental and the reconstructed temperature records is not known. As a hypothesis, the sun's magnetic field, which is correlated with sunspot numbers, is put forward as an explanation. The long-term low-frequency fluctuations in sunspot numbers are not detectable by the DFA in the monthly instrumental records, resulting in the common low Hurst exponents. The same does not hold true for the 2000-year-long reconstructed records, which explains both their higher Hurst exponents and the higher probabilities of strong 100-year temperature fluctuations. A long-term synthetic record that embodies the reconstructed sunspot number fluctuations includes the different Hurst exponents of both the instrumental and the reconstructed records and, therefore, corroborates the conjecture.

Key words: northern hemispheric 100-year temperature fluctuations, persistence of temperature records, proxy temperatures from stalagmites and tree rings, solar influence.

1 Introduction

It is widely assumed that the warming of the northern hemisphere during the 20th century was anomalous. Greenhouse gases are indeed an agent of warming, however, exactly by how much they contributed to the 20th century rise in temperature and hence can be linked to human influence, remains an issue that has yet to be settled. The literature refers to this as the 'detection and attribution problem' [1], [12], [13], [47], [60], [59]. In most of the papers discussing this problem, monthly local records of up to 120 years were consulted. Some use a mixture of global and local records. Up to 95 instrumental records going back 50 to 120 years from stations all over the globe were explored but indications of a warming of the atmosphere could not be found in the vast majority of cases [7]. A totality of 17 local records and 15 global records from all over the world were examined for both the recent 50-year and the longer 100-year period, as well as a further 13 local records from different parts of the world for the last 50 years only [26]. The authors found only weak support for the thesis that the warming trend in the last 50 years changed its character compared with the first 50 years of the 20th century.

Compared with the 20th century, a different picture arises at the end of the 18th century because all reliable instrumental temperatures for the northern hemisphere - there are no records for the southern hemisphere that go far enough back in time - show a 100-year-long decline during the 19th century, turning into the better-known, recent centennial rise at the end of it. Both rise and fall are of similar magnitude. Therefore, if the 20th century temperature rise is considered to be deterministic, the same should apply to the fall in the 19th century. If we assume anthropogenic CO₂ to be the agent behind the 20th century rise, we face a problem when it comes to the 19th century.

Additional information about temperature trends of 100 years duration is derived from reconstructed temperatures as 'proxies', here from tree rings and stalagmites. Tree rings reflect the age of a tree in yearly steps, and the thickness of the rings yields information about the annual mean temperature [9]. In the thin layers of stalagmites, the age of the layer is determined by the Th/U method, and the annual mean temperature of the layer is deduced from the ¹⁸O value [38]. Two high-quality proxies, one from tree rings and the other from a stalagmite, are analyzed here. Both records go back about 2000 years and show during this period even stronger 100-year-long temperature rises and falls than prevailed in the 19th and 20th century. Hence, the cause of both the 100-year-long temperature changes during the last 2000 years and the 20th century warming remains to be discovered.

Temperature series are persistent - other notations are 'long-term correlated' or 'long-term memory' -, which is a well-known phenomenon. A warm day is more likely to be followed by another warm day than by a cold day, and vice versa. Short-term persistence of weather states on a time scale of about one week is caused by general weather situations. Longer-term persistence over several weeks is generally caused by blocking situations that arise when a high pressure system remains in place for many weeks. Persistence over many months, seasons, years,

decades, and even longer periods is usually associated with anomaly patterns in sea surface temperatures, and even with the influence of long-term variations in the activity of the sun, but there is no universal explanation that can be used in all cases [5], [6], [42], [45], [50].

In long-term correlated temperature series $T_i, i = 1, \dots, N$ the autocorrelation function

$$C(s) = \frac{1}{\sigma_N^2 (N - s)} \sum_{i=1}^{N-s} (T_i - \langle T \rangle_N)(T_{i+s} - \langle T \rangle_N) \quad (1)$$

decays with increasing s according to the power law

$$C(s) \sim s^{-\gamma} \quad (2)$$

where $\langle T \rangle_N = 1/N \sum_{i=1}^N T_i$ is the average of the T_i , s is the time lag, and σ^2 is the variance. Typical values for the exponent in Eq. (2) are arranged between $0.4 < \gamma < 0.8$.

However, the most important characteristic of long-term correlated records is that they include natural fluctuations that appear to be trends caused by external impacts. Figure 1 depicts an example.

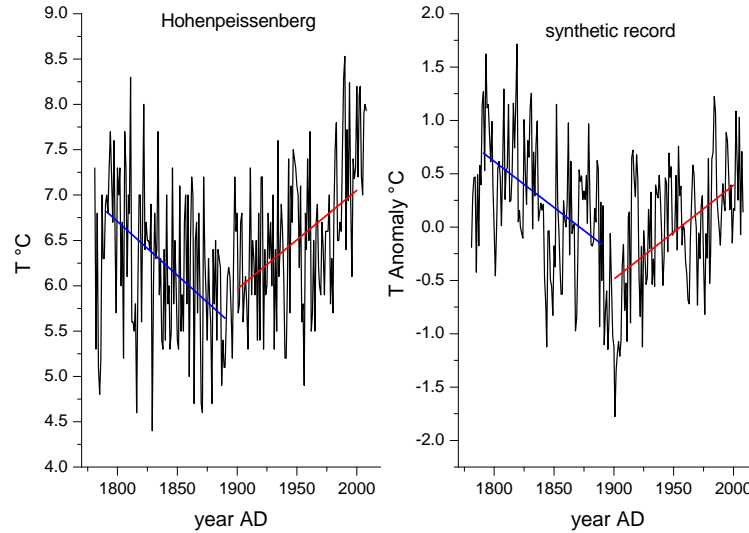


Fig. 1. (Color online) Comparison of the Hohenpeissenberg temperature record for the period 1781-2008 (left panel) with a synthetic record (right panel). The ostensible trends for the years 1789-1890 and 1901-2000 are similar in both temperature series. However, the synthetic record is purely long-term correlated without any deterministic trend.

The synthetic record shows apparently similar 100-year-trends as for the Hohenpeissenberg series, but the synthetic data are only long-term correlated. As a consequence, conventional methods based on moving averages can no longer be used with persistent records to separate deterministic trends from natural fluctuations. Additionally, in persistent records often a clustering of extreme events that is, in reality, quite natural will seem to be caused by an external trend [2], [4], [8]. Long-term correlations were not only detected in temperature series, they are ubiquitous in nature at all time scales. Among others, persistence was found in hydrological records, economic records, physiological records, and earthquake events [3], [8], [15], [16], [17], [18], [25], [29], [30], [37], [40], [48], [49]. Therefore, the power law of Eq. (2) characterizes the behaviour of persistent records quite generally.

2 Methods: Detrended fluctuation analysis

In this paper, linear regression lines are used for the analysis of temperature series. A temperature rise or fall Δ_i is here generally due to the (backward) linear regression line for the 100 annual temperatures T_{i-99}, \dots, T_i . Following [26], the dimensionless, relative temperature change Δ_i/σ_t with σ_t as the standard deviation around the regression line is considered as the gauge for temperature changes (the common standard deviation, which can be affected by an external trend is not feasible here). The temperature records that are analyzed in this article are available as medium-range monthly instrumental records and as annual long-range reconstructed records from tree rings and stalagmites. From the monthly data, the seasonal effects have to be eliminated. At this, for each calendar month the mean value of the whole record is subtracted from the data and divided by the seasonal standard deviation yielding the normalized record $T_i, i=1, \dots, N$ that will be applied in the further analysis.

In the following, the DFA (and FA) of temperature records is described. If temperature records contain external trends, the exponent γ in Eq. (2) has not the correct value. Furthermore, the direct calculation of $C(s)$ by Eq. (1) is affected by side effects, for instance, the shortness of the record, and by deterministic trends [27]. Several methods to solve these problems have been propagated, the fluctuation method (FA), the detrended fluctuation method (DFA) and wavelet analysis [4], [7], [10], [16], [19], [23], [46], [48], [49], [54], [55], [58]. However, in particular the DFA yields correct results if the record contains external trends. For a start, the basic fluctuation analysis FA forms the following profiles as sums over the normalized temperatures T_i :

$$Y_j = \sum_{i=1}^j T_i \quad j = 1, \dots, N \quad (3)$$

Furthermore, it establishes the standard deviation $F(s)$:

$$F(s) = \sqrt{\frac{1}{(N-s)} \sum_{j=1}^{N-s} (Y_{j+s} - Y_j)^2} \quad (4)$$

For long-term correlated data $F(s)$ of Eq. (4) scales with a power law

$$F(s) \sim s^\alpha \quad (5)$$

The exponent α in Eq. (5) is linked to the power law of Eq. (2) by

$$\begin{aligned} \alpha &= 1 - \gamma/2 & \text{for } 0 < \gamma < 1 \\ \alpha &= 0.5 & \text{for } \gamma \geq 1 \end{aligned} \quad (6)$$

[16]. The exponent α is usually referred as Hurst exponent, because Hurst was the first who detected long-term correlation in time series, but he used a different method - the rescaled range (RS) analysis [14]. Due to the already denoted limits of γ together with Eq. (6), α has the limits $0.5 \leq \alpha < 1$, where $\alpha = 0.5$ stands for complete randomness, and $\alpha \approx 1$ for very strong persistence. For $\alpha > 1$, the record becomes unsteady.

The detrended fluctuation analysis DFA can be seen as an advanced FA, which automatically eliminates trends of the polynomial order ν from the profile Y_j and - because Y_j in Eq. (3) integrates the record $\{T_i\}$ - of polynomial order $(\nu - 1)$ from the record itself. In DFA_ν , the profile Y_j of Eq. (3) is divided into $N_s = \text{int}(N/s)$ non-overlapping intervals of equal length s , and in each interval a polynomial P_ν of order ν is evaluated, which provides the best fit for the profile Y_j . Generally, a short segment at the end of the profile remains. In order not to neglect this segment, one repeats the same procedure from the other end of the record resulting in $2N_s$ segments. In the next step the new profile Z_j replaces Y_j of Eq. (3):

$$Z_j = Y_j - P_\nu \quad (7)$$

Finally, with $G_k^2(s) = \frac{1}{s} \sum_{j=(k-1)s+1}^{ks} (Z_j)^2$ the new $F_\nu(s)$ replaces $F(s)$ of Eq. (4):

$$F_\nu(s) = \sqrt{\frac{1}{2N_s} \sum_{k=1}^{2N_s} G_k^2(s)} \quad (8)$$

In this study, only DFA_2 is used. For purely long-term correlated data, the fluctuation function $F_\nu(s)$ scales like $F(s)$ in Eq. (5) with the same exponent α . It is useful to depict $F_\nu(s)$ as function of s in a log-log diagram, which enables the exponent α to be easily evaluated. It should be stressed that Eq. (5) as well as the former Eq. (2) expresses the fact that a consistent scaling behavior is induced by the numerous mechanisms that generate persistence in temperature records. Consequently, neither Eq. (2) nor a power law of the FA or DFA says anything about its origin.

In principle, the power law of Eq. (5) does not depend on the time scale of s - whether monthly or yearly. A minimum of $\nu + 2$ data points are needed for the fit procedure with polynomials of order ν , and for this reason, the $F_\nu(s)$ graph begins with $s_{min} = \nu + 2$. A minimum of about $N = 600$ data points T_i are required to get reliable results from DFA. Consequently, monthly not

annual data are indispensable for the FA and DFA of instrumental temperature records with 250 years length at the most. Furthermore, reliable DFA results are confined to a maximum of $s \approx N/4$ because otherwise the number of intervals $N_s = \text{int}(N/s)$ becomes too small. Lastly, in $F_2(s)$ the interval length s is too small for about the first five s values, and due to numerical effects, the Hurst exponent becomes slightly too high in this domain. This reveals every double-logarithmic $F_2(s)$ plot as a weak dip for a few of the first s values (see Figure 4 in paragraph 4 as an example). To summarize, DFA is reliable within

$$s_{\min} + 5 \leq s \leq N/4 \quad \text{and} \quad N \geq 600 \quad (9)$$

3 Methods: Exceedance probabilities

In the following, the probability that in a long-term correlated record with a Hurst exponent α the temperature change Δ of a linear regression line over 100 years appears naturally is of main interest. 'Natural' denotes that there is no external trend in the record. Following [26], [28], [34] $W(\Delta/\sigma_t, \alpha)$ indicates for a fixed Hurst exponent α the exceedance probability that values of $\geq \Delta/\sigma_t$ over 100 years occur naturally. $W(\Delta/\sigma_t, \alpha)$ is not restricted to positive Δ/σ_t . If one begins, by definition, with cooling, the exceedance probability converges to the theoretical limit of $W = 1$ for extremely strong negative Δ/σ_t values and decreases with rising Δ/σ_t . In natural records we have equal fractions with warming and cooling, hence for all α values $W(0, \alpha) = 0.5$ is valid. To give further examples, $W(-2, 0.7) = 0.9954$, $W(-0.8, 0.7) = 0.849$, $W(-0.3, 0.7) = 0.65$, $W(0, 0.7) = 0.5$, $W(0.3, 0.7) = 0.35$, $W(0.8, 0.7) = 0.151$, and $W(2, 0.7) = 0.0046$ hold - by using later Eq. (11). The general relation

$$W(-\Delta/\sigma_t, \alpha) = 1 - W(\Delta/\sigma_t, \alpha) \quad (10)$$

confirms congruent fractions with positive and negative Δ/σ_t values in natural records. If values of W over 0.5 belong to cooling, then, for instance, an exceedance probability of 0.9 would be as significant as of 0.1 for warming.

The latest method to evaluate the exceedance probabilities $W(\Delta/\sigma_t, \alpha)$ for natural records of a fixed α in a systematical way is a combination of DFA, synthetic records, and Monte Carlo simulations [26], [28]. This method generates large - generally $2^{21} = 2,097,152$ data points in length - long-term correlated synthetic records with this Hurst exponent α and evaluates from these long records n short sub sequences for the period under consideration, in our case 100 years, each with the same local α (in general, the α values of sub sequences are similar but in general not identical with the α of the long record). For statistical reasons, the number n must be sufficiently large. In the stack of n synthetic records, the number z of records with warming equal to or higher than $\Delta/\sigma_t > 0$ is counted. As a result, the fraction z/n yields the exceedance probability $W(\Delta/\sigma_t, \alpha)$ for positive Δ/σ_t values in natural records. By systematically varying Δ/σ_t and α the results can be expressed empirically by the following analytic approximation

for $\Delta/\sigma_t > 0$ [26]:

$$W(\Delta/\sigma_t, \alpha) = C \cdot \exp[-B(\alpha)(\Delta/\sigma_t - 0.2)] \quad (11)$$

For a period of 100 years the following parameters are valid: $C = 1.15$; $B(\alpha) = D\alpha^{-\delta}$ with $D = 1.26$, $\delta = 2.5$ [26]. Eq. (11) holds for $W \leq 0.1$. For $W > 0.1$, a continuation of Eq. (11) is yielded using the error function [26]. For simplicity, this continuation is included if Eq. (11) is referred to. The approximation of Eq. (11) is completed for negative values of Δ/σ_t by Eq. (10). It is demonstrated, for instance, if we were to choose $\Delta/\sigma = 1$ and $\alpha = 0.8$, Eq. (11) yields the exceedance probability $W(1, 0.8) = 0.16$ and furthermore by applying Eq. (10) of $W(-1, 0.8) = 0.84$. Hence, the 16% percentage of long-term correlated or detrended real records with $\alpha = 0.8$ and 100 years in length shows warming at magnitudes $\geq (\Delta/\sigma = 1)$. Further, the 84% percentage of records shows a relative temperature change $\geq (\Delta/\sigma = -1)$ and, conversely, the 16% percentage of records a cooling at magnitudes $\leq (\Delta/\sigma = -1)$. W can increase by several orders of magnitude when α increases. As a consequence, an increase of $\Delta/\sigma_t > 0$, which is very unlikely for small α values, becomes quite normal for larger ones. To give an example, $\alpha = 0.6$ yields $W(1.5, 0.6) = 0.003$, but for $\alpha = 0.8$ this value increases to $W(1.5, 0.8) = 0.66$.

The use of the approximation in Eq. (11) for the analysis of real temperature records that are detrended by DFA is based on the hypothesis that real records are long-term correlated with an additional trend. Furthermore, for a reliable analysis, the trend is assumed to be linear. In order to distinguish between a natural fluctuation and an external trend, a confidence level "a" is needed. Consequently, the domain $0 < W < a$ of warming and $(1 - a) < W < 1$ of cooling is considered to include external trends. On the other hand, relative trends in the $(1 - 2a)$ confidence interval $a \leq W \leq (1 - a)$ are regarded as natural. It is defined - to some extent subjectively - the confidence level of 0.025, which corresponds to a confidence interval of $(1-2a) = 0.95$ in accordance with general practice.

4 Application: Medium-range monthly instrumental temperature records

Medium-range monthly instrumental records going back more than 200 years exist only for stations in the northern hemisphere. But even here they are not abundant. The places with reliable monthly temperature series number five in all: Prague, Hohenpeissenberg, Vienna, Paris, and Munich, and they have some of the longest, most reliable (and available) instrumental temperature records to be had anywhere. In Table 1 their characteristics are cited. They go back for somewhat more than 220 years, with the earliest being 1757 for Paris and the latest starting in 1781 in Hohenpeissenberg and Munich and can be accessed at [11], [22], [43], [57]. The related temperature courses are shown in Figure 2.

Station	Period	Data consistency
Hohenpeissenberg	1781-2008	complete
Munich-Riem	1781-2009	1992-2009 data from Munich airport
Prague-Klementinum	1770-2009	complete
Paris-le-Bourget	1757-2008	1994-2009 data from Paris waterworks
Vienna	1775-2008	complete

Table 1: Medium-range monthly temperature records analyzed in this study

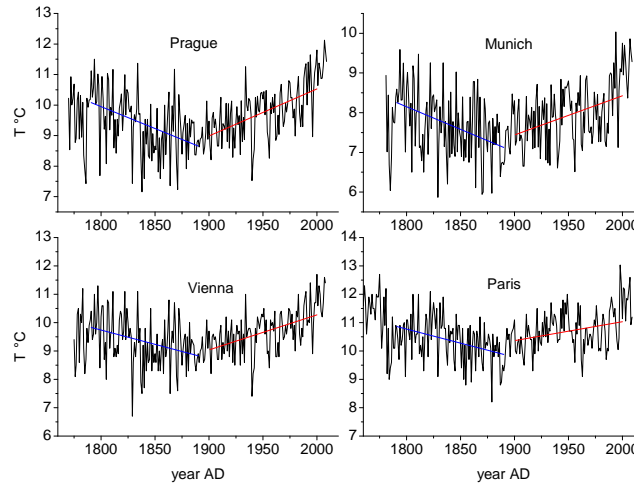


Fig. 2. (Color online) Temperature courses for Prague, Munich, Vienna, and Paris with 100-year linear regression lines for 1791-1890 and 1901-2000 (the temperature course of Hohenpeissenberg was already depicted in Figure 1 of paragraph 1).

The periods 1791-1890 and 1901-2000 were selected as having for all stations roughly the steepest temperature fall and temperature rise during the last 220 years. All the records show the same general behavior: a temperature drop in the period 1791-1890 and a rise for 1901-2000 with both roughly the same magnitude.

The following Figure 3 depicts the values of Δ_i/σ_t with Δ_i as the temperature difference due to the 100-year linear regression line through the data points T_{i-99}, \dots, T_i and σ_t as the appropriate standard deviation around the line. The yearly indices i are moving earliest from the year $(1757 + 99)$ until latest 2008 or 2009 (see Table 1). The dashed line $\Delta_i/\sigma_t = 2$ in Figure 3 is for comparison with later Figure 6, which will reveal that the relative 100-year temperature rises Δ_i/σ_t in the last 2000 years were often far stronger than the appropriate rises of the 20th century.

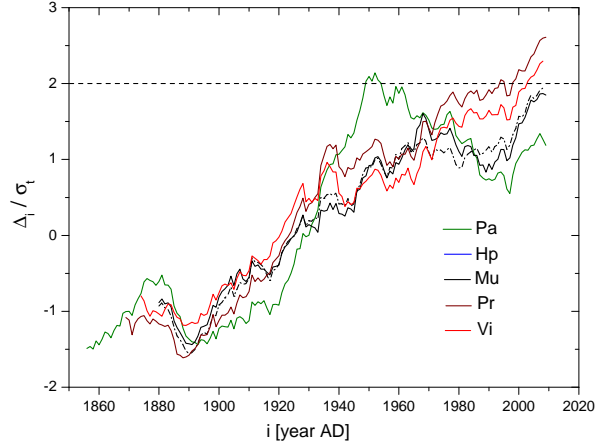


Fig. 3. (Color online) Δ_i/σ_t against years i , with Δ_i as the rises and falls of the (backward) 100-year linear regression lines through the temperatures T_{i-99}, \dots, T_i and σ_t as the standard deviation around the lines, for the medium-range series (top to bottom) Pa = Paris, Hp = Hohenpeissenberg, Mu = Munich, Pr = Prague, and Vi = Vienna. With few exceptions, $\Delta_i/\sigma_t \leq 2$ holds for all years ≤ 2000 (dashed line).

Figure 4 depicts the $F(s)$ graphs of the FA in Eq. (4) and the $F_2(s)$ graphs of the DFA2 in Eq. (8) for the instrumental series. All the graphs have a common shape. The numerical effect of the somewhat greater Hurst exponents on a few of the first s values has already been discussed in paragraph 2. A slight $F_2(s)$ deviation for the DFA2 graph of Paris shows a weak cross-over at about 600 months (50 years). Figure 4 reveals that $\alpha > \alpha_2$ holds for all records, which is an indication that linear trends in the records have been eliminated by DFA2. Table 2 shows the appropriate numerical results for α from the fluctuation analysis (FA) and for α_2 from the detrended fluctuation analysis (DFA2). With the exception of Munich and Hohenpeissenberg in the period 1791-1890, Table 2 exhibits that for all records and all periods, $\alpha > \alpha_2$ is valid, indicating that linear trends have been removed from the records by DFA2. The values of Δ_i , Δ_i/σ_t , and σ_t are cited in Table 3 for the periods 1791-1890 and 1901-2000. Further, the exceedance probabilities $(100 - W)$ for cooling and W for warming (in percent) derived from Eqs. (10)-(11) are given.

Within the already noted confidence interval of 95%, the exceedance probabilities in column 5 and column 9 of Table 3 are arranged in the trend domain of $W > 97.5\%$, i.e. $(100 - W) < 2.5\%$ for cooling and $W < 2.5\%$ for warming. This holds for both centennial occurrences and, therefore, both have to be judged as nonnatural - with the only exception of Vienna for the period 1791-1890.

	α	α_2	α	α_2	α	α_2
	1791- 2000	1791- 2000	1791- 1890	1791- 1890	1901- 2000	1901- 2000
Munich	0.69	0.63	0.63	0.66	0.66	0.62
Hohenpeis.	0.67	0.60	0.61	0.63	0.67	0.59
Prague	0.75	0.61	0.74	0.66	0.71	0.63
Paris	0.71	0.57	0.71	0.61	0.63	0.52
Vienna	0.72	0.59	0.67	0.66	0.69	0.59

Table 2: Hurst exponents α of the FA and α_2 of the DFA2 with the applied time periods. The appropriate graphs are depicted in Figure 4.

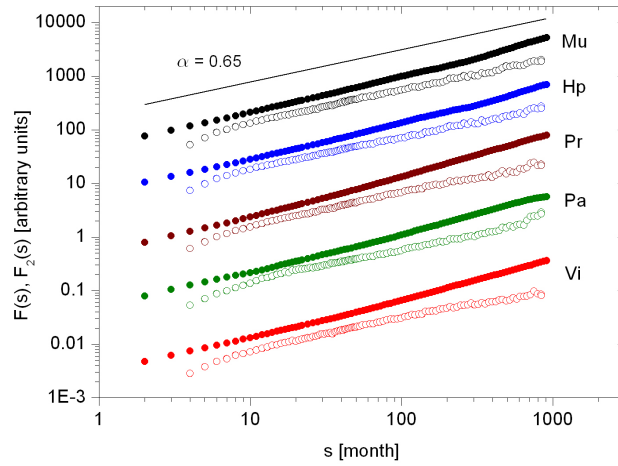


Fig. 4. (Color online) $F(s)$ of the FA, shown as filled circles and $F_2(s)$ of the DFA2, shown as open circles for the records (top to bottom) Mu = Munich (black), Hp = Hohenpeissenberg (blue), Pr = Prague (brown), Pa = Paris (green), and Vi = Vienna (red) for the period 1791-2000 in a double-logarithmic plot, and with the graphs shifted for clarity. Obviously, all records show persistence over more than 50 years. The related Hurst exponents α derived from FA and α_2 from DFA2 are cited in Table 2. The appearance of $\alpha > \alpha_2$ in all records indicates that DFA2 has removed linear trends from all of them. The line with $\alpha = 0.65$ is for comparison.

We do not know what caused these two centennial occurrences in opposite direction. Consequently, if we would suppose anthropogenic CO_2 as an agent for the recent warming we are faced with the problem when we look for the agent of the cooling in the period 1791-1890. A further aspect worth mentioning is that

the standard deviations for 1791-1890 are generally higher than for 1901-2000. The reason for this difference is also not known.

In particular for the last 50 years, instrumental temperatures in populated areas are subject to the urban heat island effect (UHI) and further warm bias. However, no such effects are considered here. It should be emphasized that taking warm bias into account would enforce the sought-after unbiased temperature falls for the 19th century and have a dampening effect on the unbiased 20th century rise caused by anthropogenic green house gases.

	Δ_{1890} [°C]	Δ_{1890}/σ_t	σ_t [°C]	100- W_{1890} [%]	Δ_{2000} [°C]	Δ_{2000}/σ_t	σ_t [°C]	W_{2000} [%]
Munich	-1.14	-1.43	0.79	1.4	0.99	1.46	0.67	0.6
Hohenp.	-1.19	-1.54	0.76	0.5	1.09	1.56	0.69	0.2
Prague	-1.44	-1.57	0.91	0.9	1.54	2.17	0.71	< 0.1
Paris	-0.99	-1.36	0.72	0.7	0.67	1.03	0.64	0.5
Vienna	-1.01	-1.17	0.86	3.6	1.23	1.89	0.65	< 0.1

Table 3: Δ_{1890} in column 2 denotes the temperature fall of the linear regression line for the 100-year period 1791-1890. The columns 3, 4, and 5 show Δ_{1890}/σ_t , σ_t as the standard deviation around a regression line, and $(100 - W_{1890})$ with W_{1890} as the exceedance probability in percent that temperatures during the period 1791-1890 with values $\geq \Delta/\sigma_t$ occur in the DFA-detrended record naturally. Columns 6 - 9 give the analogous results for the 100-year temperature rise of the period 1901-2000.

5 Application: Reconstructed long-range annual records

Two long-range annual records, which are depicted in Figure 5 were considered in this letter: a stack about tree rings and further biological proxies [43], referred to here as MOB, and the SPA12 record of stalagmites [38]. MOB covers the period 0 - 1979 AD and is a composition derived from wavelet analyses of 11 low-resolution series - ice from boreholes, Foraminifera and stalagmites - and 7 tree ring proxies with annual or decadal time resolutions found in different sites of the northern hemisphere [41]. MOB is not local and therefore an exception to all other records analyzed in this paper. In the case of SPA12, the dated isotopic composition of a stalagmite from the Spannagel Cave at 2347 meter above sea level in the Central Alps near Innsbruck was translated into a highly resolved record of temperatures during the past 2000 years [38]. SPA12 goes from -90 to 1935 AD, and the average time resolution is slightly over one year, with a minimum of 0.56-year- and a maximum of 10-year steps (10-year steps in only 9 cases). For the purpose of the DFA analysis, SPA12 was standardized here to one-year steps by Spline interpolation. After this standardization no differences to the original record could be detected by eye, and no differences in the later DFA analysis were found by using interpolations with different Spline functions. The variance $var = 0.048$ of MOB is smaller than the variance $var = 0.345$ of SPA12. As a further comparison, the annual mean temperature inside the Spannagel cave was instrumentally evaluated as 1.8 °C for the year 2003 alone [38].

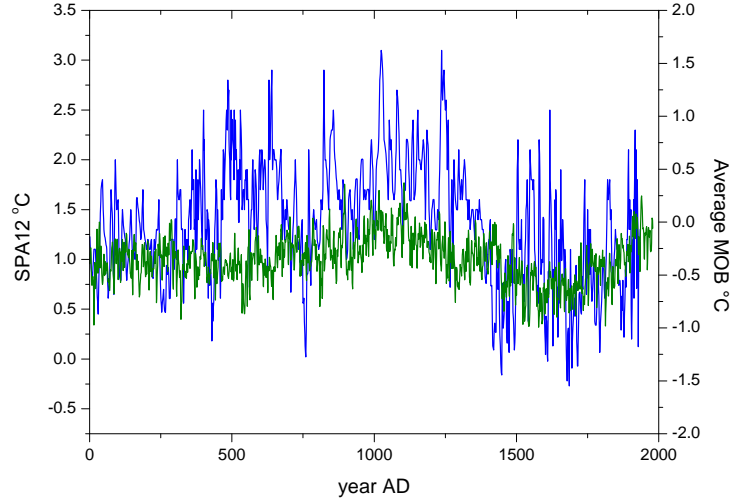


Fig. 5. (Color online) Reconstructed long-range annual records, SPA12 (blue) from a stalagmite and MOB (green) from a stack of tree rings in the northern hemisphere and further biological proxies (as an anomaly). The variance of MOB is roughly seven times smaller than for SPA12. In both records, the medieval warm period and the Maunder Minimum can be clearly identified.

A comparison of tree rings and additional biological proxies with SPA12 is discussed in [38], [39]. The uncertainty of the SPA12 temperatures is indicated to be ± 0.3 °C in [38], and ± 0.4 °C for MOB in [41]. The most conspicuous difference between stalagmite and tree ring proxies has to do with the variance. It is reported that smoothed MOB and SPA12 curves are also in accordance with other biological proxies and with a combined temperature reconstruction of Greenland ice cores and tree rings from Scandinavia and Siberia [36]. In [38], a comparison of the smoothed SPA12 record with a sea surface temperature (SST) model curve of the Bermuda Rise yielded by [33] is depicted that also shows reasonable accordance. Further, a comparison of SPA12 with an annual winter curve of the Alps is given in [36]. However, it is known that the thickness of tree rings depends not only on the annual mean temperatures, but also on precipitation. Similar problems are reported for stalagmites [38], [39]. As a consequence, short time periods show a lack of congruence between MOB and SPA12 as well as between the different tree ring proxies themselves [47].

Figure 6 shows the 100-year (left panel) and the 500-year (right panel) events Δ_i/σ_t , with Δ_i as the rise or fall of linear regression lines on the time intervals $[i-99, i]$ resp. $[i-499, i]$ for SPA12 and MOB. In the 100-year cases, Δ_i/σ_t values of > 2 and < -2 are commonplace during the last 2000 years (see dashed line

for comparison). Conversely, all instrumental medium-range records before the year 2000 have $|\Delta_i/\sigma_t|$ values of about 1.5, with a maximum for Prague as the single exception (see Figure 3 and Table 3). This in itself indicates that neither the 19th century fall nor the 20th century rise in temperature are exceptional in the long run. Concerning the 500-year graphs, the right panel of Figure 6 depicts additionally the 500-year $\Delta\text{SSN}_i/\sigma_t$ of the annual SSN sunspot number record for comparison (see paragraph 6 for relevance).

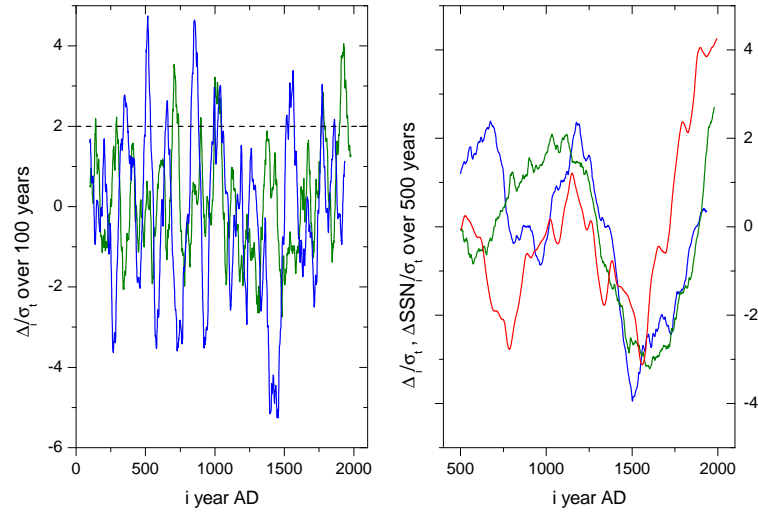


Fig. 6. (Color online) Left panel: Δ_i/σ_t , with Δ_i as the rise or fall of 100-year linear regression lines for the temperatures on the time intervals $[i-99, i]$ and σ_t as the standard deviation around the lines, for SPA12 (blue) and MOB (green). Values of $\Delta_i/\sigma_t > 2$ are quite common during the last 2000 years (dashed line for comparison). Right panel: analogous to the left but shows the 500-year events Δ_i/σ_t for SPA12, MOB and, as a further comparison, the $\Delta\text{SSN}_i/\sigma_t$ (red) of the yearly sunspot number record SSN (see paragraph 6 for relevance).

Figure 7 (left panel) depicts the $F(s)$ and $F_2(s)$ graphs of the FA and DFA for SPA12 and MOB. The evaluated Hurst exponents are $\alpha = \alpha_2 = 0.95 \pm 0.02$ for SPA12 and $\alpha = \alpha_2 = 0.85 \pm 0.02$ for MOB. The relevance for the further graphs in the left panel of Figure 7 will be given in Eq. (12). In the case of MOB, the Hurst exponent α_2 from DFA has already been evaluated as $\alpha_2 = 0.86 \pm 0.02$ in [47]. The right panel of Figure 7 shows the observed exceedance probabilities W for $\Delta/\sigma_t > 0$ and $(1-W)$ for $\Delta/\sigma_t < 0$ of both SPA12 and MOB together with the theoretical curve for the Hurst exponent $\alpha = 0.95$ derived from Eq. (11).

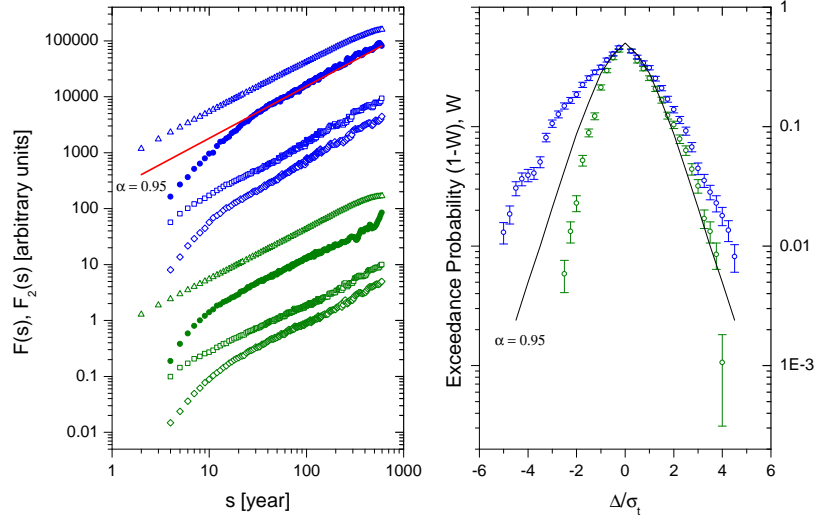


Fig. 7. (Color online) Left panel from top-down, with plotted curves shifted for clarity; blue triangles: $F(s)$ of the FA for SPA12; blue filled circles: $F_2(s)$ of the DFA2 for SPA12; blue squares: $F_2(s)$ of the DFA2 for a synthetic SPA12 record (see Eq. (12) for relevance); blue diamonds: $F_2(s)$ of the DFA for a synthetic SPA12 record with additional extreme short-term persistence. Below this, the same graphs are repeated in green for MOB. The red line with $\alpha = 0.95$ is for comparison. Right panel: observed exceedance probabilities for SPA12 (blue) and MOB (green) together with the theoretical curve of Eq. (11) for $\alpha = 0.95$. $(1-W)$ refer to negative values of Δ/σ_t , W to positive ones. For warming, the observed W values match roughly the theory, but the cooling domain shows aberrations.

Because $\alpha = \alpha_2$ has been evaluated for both SPA12 and MOB, no linear trends have been removed by DFA. Obviously, the Hurst exponents $\alpha_2 \approx 0.9$ for the long-range records MOB and SPA12 contradict their medium-range instrumental counterparts of $\alpha_2 \approx 0.6$ (see Table 2). As already stated, the detrended Hurst exponents do not basically depend on the time scale - months or years - and should therefore be similar for all temperature records of sites located relatively close to each other. In fact, all records in this paper - except for the MOB record - are local, and the distance between them is no more than about 1000 km at the most. Moreover, without further investigation into the reliability of the long-range reconstructed records, the discrepancies in the DFA results between the medium- and long-range records cannot be explained. As Figure 7 demonstrates, the $F_2(s)$ graphs for SPA12 and MOB (filled circles) exhibit an unusual downward dip for about $s < 20$ years that exceeds the weak numerical effect already discussed. In an attempt to gain more insight here, a simulation

was carried out by synthetic records of p_i with a Hurst exponent $\alpha_2 = 0.95$, simulating SPA12, and m_i with $\alpha_2 = 0.85$, simulating MOB. As expected, the $F_2(s)$ graphs of both synthetic records p_i and m_i (open squares in Figure 7) showed only the common weak downward dip. Next, to simulate the strong downward dip, Eq. (12) was introduced to furnish the additional conditions for p_i and m_i :

$$\begin{aligned} \bar{p}_{i+2} &= p_i + p_{i+1} + p_{i+2}, & i &= 3, \dots, 1933 \\ \bar{m}_{i+2} &= m_i + m_{i+1} + m_{i+2}, & i &= 3, \dots, 1977 \end{aligned} \quad (12)$$

This provides \bar{p}_i and \bar{m}_i , which yield accordance (open diamonds in Figure 7). An explanation of the strong downward dip might be that the effective time resolution of both SPA12 and MOB is in reality about 3-4 years, while the reconstructed temperature for each year is a 3-4 year mean. A similar dip on $F_2(s)$ graphs in sea surface temperature (SST) records was found and the hypothesis advanced that it has to do with the influence of the North Atlantic Oscillation (NAO) and the El Niño southern oscillation [42].

6 A hypothesis on the sun's influence

Because no artifacts are known that could be responsible for a strong persistence lasting at least 600 years in both tree ring and stalagmite proxies (see left panel of Figure 7), another agent may be supposed. For this purpose, a reconstructed sunspot number record was used [52]. This covers more than 10,000 years (from -9455 to 1895 AD) in 10-year time steps. Direct sunspot number observations (Wolf numbers) as yearly averages for the period 1700 - 1995 AD provided additional support [44]. This completed record has been given the name 'SSN' here, and covers a total of 11,450 years. It is used in smoothed 10-year steps. Annual and monthly records are calculated from it by Spline interpolation. The left panel of Figure 8 shows the SSN from 0 to 1995 AD. The right panel depicts the DFA2 result for SSN, with 10 years steps and for the whole record length of 11,450 years (smaller time steps for SSN do not change the DFA2 result significantly). Apparently, the $F_2(s)$ curve for DFA2 in Eq. (8) does not follow the scaling law of Eq. (5). As already stressed, there is an obvious conflict between the Hurst exponents $\alpha_2 \approx 0.6$, derived from the instrumental data (see Table 2 and Figure 4 in paragraph 4), and $\alpha_2 \approx 0.9$, derived from the reconstructed temperatures for SPA12 and MOB (see Figure 7 in paragraph 5). This paper advances the hypothesis of fluctuations in sunspot numbers, which are depicted in the left panel of Figure 8 as an agent here. The sun's magnetic field modulates the cosmic ray flux hitting the earth. Both cloud generation by cosmic rays and Earth temperatures are the subject of intense discussion [20], [21], [24], [31], [32], [35], [50], [51], [52], [53], [56].

The reconstructed sunspot number record SSN in Figure 8 is a visual representation of this presumed mechanism. The relatively slow fluctuations in sunspot numbers - as opposed to the fast fluctuations in monthly temperatures - act as a deterministic trend over the last two hundred years that is roughly linear for the short intervals of 20 to 50 years.

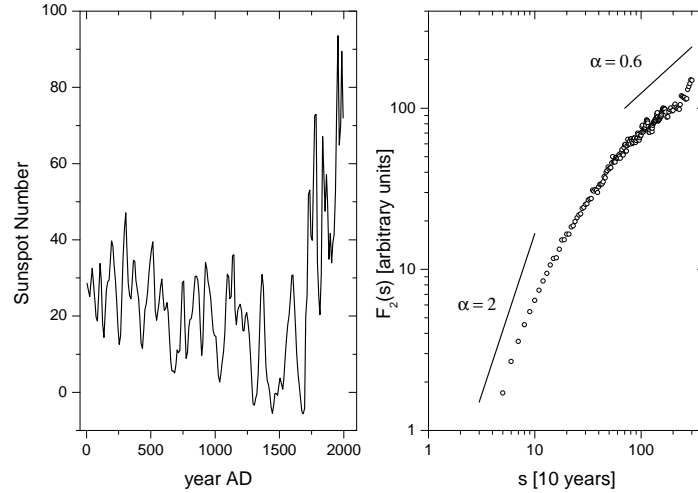


Fig. 8. (Left panel: sunspot number record SSN during the last 2000 years. Right panel: $F_2(s)$ from DFA2 for the SSN sunspot number record from -9455 AD to 1895 AD in 10-year steps. $F_2(s)$ does not take the usual scaling behaviour of $F(s) \sim s^\alpha$ of Eq. (5) for long-term correlated records, but instead shows a sliding gradient without any distinctive cross-over before $s = 3000$ years. The s values up to about 100 years have an $\alpha_2 \approx 2$, which drops down to $\alpha_2 \approx 0.6$ for $s > 1000$ years. The lines with $\alpha = 2$ and $\alpha = 0.6$ are for comparison.

In the medium-range records, the SSN trend is therefore identified as linear by DFA2 and is removed, which explains the low detrended Hurst exponents. However, in the long-range SPA12 and MOB records, the fluctuations in SSN are not linear, and are, therefore, not removed by DFA2. Consequently, they increase the Hurst exponent. The sunspot number hypothesis claims that the instrumental records would also reveal greater Hurst exponents provided that they were well over 250 years in length. Unfortunately, no such records exist. This means that the hypothesis could only be tested on synthetic records. A 17,880 month (1490 years) synthetic record x_i with a Hurst exponent of $\alpha = 0.6$, simulating the medium-range instrumental records, was generated and superimposed on the monthly sunspot number record ssn_i . This ssn_i was established from the part of SSN that corresponds to the time interval 505 - 1995 AD by applying Spline interpolation and normalization. The superimposition is carried out by means of

$$css_i(\xi) = (1 - \xi) x_i + \xi \cdot ssn_i \quad i = 1, \dots, 17880 \quad [months] \quad (13)$$

This results in the combined record $css_i(\zeta)$ with a temporarily unknown factor ζ and is referred to here as CSS.

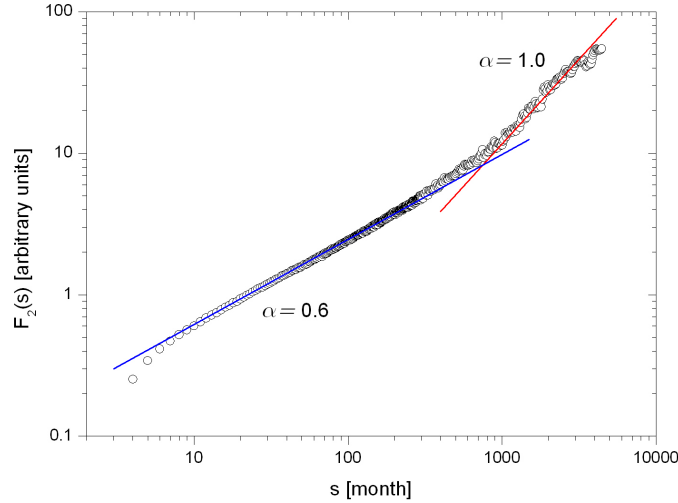


Fig. 9. (Color online) $F_2(s)$ graph of the detrended fluctuation analysis (DFA2) for the combined monthly record CSS of Eq. (13) over a total period of 17,880 months (1490 years). The cross-over at about 700 months (≈ 60 years) indicates a lower limit for a possible detection of the sun's influence by DFA2 in the medium-range records. On the left of it, the Hurst exponent α_2 corresponds to the medium-range instrumental records at $\alpha_2 \approx 0.6$ (see Figure 4 and Table 2 in paragraph 4) and, on the right, to the long-range records SPA12 and MOB at $\alpha_2 \approx 0.9$ (see Figure 8 in paragraph 5). Because the reliability of DFA for monthly records of 200 years in length is restricted to about 50 years, the instrumental records are too short to reveal the cross-over.

The first month in Eq. (13) corresponds to the year 505 AD and $i = 17,880$ corresponds to 1995 AD. Eq. (13) follows the method of superimposing trends on synthetic records [49]. Because the sunspot hypothesis demands that CSS shows both the features of the medium-range and long-range records, a value $\zeta = 0.013$ was identified that achieves this purpose, as Figure 9 demonstrates. Figure 9 unveils a cross-over between 500 and 1000 months (40 - 80 years). On the left of it, the Hurst exponent $\alpha_2 \approx 0.6$ corresponds to the instrumental records and on the right, $\alpha_2 \approx 1$ corresponds to SPA12 and MOB. It should be pointed out that merely superimposing two synthetic records with different Hurst exponents will not show a crossover. Figure 9 provides an explanation of the different Hurst exponents in the instrumental and reconstructed records: the detrended fluctuation analysis DFA2 removes the sunspot fluctuations as linear trends from the instrumental records that results in their low Hurst exponents. It was already shown due to Eq. (9) that $F_2(s)$ is only feasible for $s \leq N/4$, hence

for monthly records that are about 220 years in length the limit of about $s = 50$ years holds. As a consequence, series that are not distinctly over 250 years long are basically too short to reveal by DFA2 the extreme long-term persistence caused by the sun. In Figure 4, in fact, no cross over is visible, except for a rather feeble one for Paris. However, in the case of the longer time frame, the situation changes. If we look at the CSS synthetic record as well as at SPA12 and MOB, the SSN sunspot numbers correspond here to a fast fluctuation, which increases the Hurst exponent α_2 and is not removed by DFA2.

7 Conclusion

Instrumental records going back a maximum of up to about 250 years from present show the temperature declines in the 19th century and the rises in the 20th to be of similar magnitudes. If we assume anthropogenic CO₂ to be the agent behind the 20th century rise, we face a problem when it comes to the 19th century. The detrended fluctuation analysis (DFA2) evaluated - for the five records selected here - very small natural probabilities for both centennial events. Therefore, the probability that they are the result of deterministic trends is high, but what actually caused the trends to be diametrically opposed remains unknown. In contrast, two high-quality long-range records, SPA12 and MOB, show frequent centennial rises and falls of equal and greater magnitudes than their shorter instrumental counterparts during the last 2000 years. Smoothed SPA12 and MOB records are reported to be in accordance with other biological proxies, indicating that centennial fluctuations at least as strong as those of the past 250 years were indeed common events. This is further confirmed by the DFA Hurst exponents of $\alpha_2 \approx 0.9$ for SPA12 and MOB that are far higher than the $\alpha_2 \approx 0.6$ of the instrumental records. As a consequence, the impact of anthropogenic greenhouse gases is most probably a minor effect and - in view of the 19th century temperature fall of similar magnitude - not appropriate as an authoritative explanation for any temperature rise in the northern hemisphere during the 20th century.

Because no reliable explanation can be given for the conflict between the different Hurst exponents and probabilities in the instrumental and reconstructed records, a hypothesis of solar influence (manifesting itself in long-term sunspot fluctuations) could be put forward to explain the contradiction. A monthly synthetic record covering about 1500 years and using a Hurst exponent of $\alpha = 0.6$, which corresponds to the instrumental records was therefore superimposed on the trend of the sunspot numbers. The DFA2 result for this combined record shows that it embodies both the short persistence of the instrumental data and the long persistence of the reconstructed data. The hypothesis expressed here suggests that the sun could be predominantly responsible for the 100-year-long rises and falls in temperature over the last 2000 years.

8 Acknowledgements

The author would like to thank S. Lennartz and A. Bunde (Department of Theoretical Physics III, University of Giessen - Germany), A. Mangini (University of Heidelberg and Academie of Sciences of Heidelberg - Germany) and K.O. Greulich (Fritz Lipmann Institute, University of Jena - Germany) for many helpful discussions, and furthermore, L. Motl for his hint about the Czech source of the Prague record.

References

1. T. Barnett et al., Detecting and attributing external influences on the climate system: A review of recent advances, *J. Clim.* **18**(9), p. 1291 (2005)
2. M.I. Bogachev, J.F. Eichner, and A. Bunde, Effect on Nonlinear Correlations on the Statistics of Return Intervals in Multifractal Data Sets, *Phys. Rev. Lett.* **99**, 240601 (2007)
3. M.I. Bogachev, I.S. Kireenkov, E.M. Nifontof, and A. Bunde, Statistics of return intervals between long heartbeat intervals and their usability for online prediction of disorders, *New Journal of Physics* **11**, 063036 (2009)
4. A. Bunde, J.W. Kantelhardt, Langzeitkorrelationen in der Natur: von Klima, Erbgut und Herzrhythmus, *Phys. Blätter* **57**, Nr. 5 (2001)
5. A. Bunde, J. Kropp, and H.-J. Schellnhuber, The science of disaster: Climate disruptions, market crashes and heart attacks, *Springer Verlag*, Berlin (2002)
6. J.G. Charney, and J. G. de Vore, Multiple flow equilibria in the atmosphere and blocking, *J. Atmos. Sci.* **36**, p. 1205 (1979)
7. J.F. Eichner, E. Koscielny-Bunde, A. Bunde, S. Havlin, and H.-J. Schellnhuber, Power-law persistence and trends in the atmosphere: A detailed study of long temperature records, *Phys. Rev. E* **68**(4), doi:10.1103/PhysRevE.68.046133 (2003)
8. J.F. Eichner, J.W. Kantelhardt, A. Bunde, and S. Havlin, Extreme value statistics in records with long-term persistence, *Phys. Rev. E.* **73**, doi: 10.1103/PhysRevE.73.016130 (2006)
9. J. Esper, E.R. Cook, and F.H. Schweingruber, Low-Frequency Signals in Long Tree-Ring Chronologies for Reconstructing Past Temperature Variability, *Science* **295**, 2250, doi: 10.1126/science.1066208 (2002)
10. K. Fraedrich and R. Blender, Scaling of Atmosphere and Ocean Temperature Correlations on Observations and Climate Models, *Phys. Rev. Lett.* **90**, 108501 (2003)
11. http://data.giss.nasa.gov/gistemp/station_data/
12. K. Hasselmann, Optimal Fingerprints for the detection of time-dependent climate change, *J. Clim.* **6**(10), p. 1957 (1993)
13. G.C. Hegerl, H. von Storch, K. Hasselmann, B.D. Santer, U. Cubasch, and P.D. Jones, Detecting greenhouse-gas-induced climate change with an optimal fingerprint method, *J. Clim.* **9**(10), p. 2281 (1996)
14. H.E. Hurst, Long-term storage capacity of reservoirs, *Transactions of the American Society of Civil Engineers* **116** (2447) p. 770 (1951)
15. P.C. Ivanov et al., Sleep-wake differences in scaling behaviour of the human heartbeat: Analysis of terrestrial and long-term space flight data, *Europhysics Letters* **48**(5), p. 594 (1999)

16. J.W. Kantelhardt, E. Koscielny-Bunde, H.H.A. Rego, S. Havlin, and A. Bunde, Detecting long-range correlations with detrended fluctuation analysis, *Physica A* **295**, p. 441 (2001)
17. J.W. Kantelhardt, Fluktuationen in komplexen Systemen (Fluctuations in complex Systems), professorial dissertation, *University Giessen* (Germany), 19. June 2004
18. J.W. Kantelhardt, E. Koscielny-Bunde, D. Rybski, P. Braun, A. Bunde, S. Havlin, Long term persistence and multifractality of precipitation and river runoff records, *Journal of Geophysical Research-Atmosphere* **111**, p. 1106 (2006)
19. A. Kirly, I. Bartos, and I.M. JAnosi, Correlation properties of daily temperature anomalies over land, *Tellus, Ser. A* **58**(5), p. 593 (2006)
20. J. Kirkby, Cosmic Rays and Climate, *European Organisation for Nuclear Research, CERN-PH-EP/2008-005* (2008)
21. J. Kirkby et al., Role of sulfure acid, ammonia and galactic cosmic rays in atmospheric aerosol nucleation, *nature* **476**, p. 429, doi:10.1038/nature10343 (2011)
22. <http://xmarinx.sweb.cz//KLEMENTINUM.xls>
23. E. Koscielny-Bunde, A. Bunde, S. Havlin, H.E. Roman, Y. Goldreich, and H.-J. Schellnhuber, Indication of a universal persistence law governing atmospheric variability, *Phys. Rev. Lett.* **81**(3), p. 729 (1998)
24. N.A. Krivova, and S.K. Solanki, Solar variability as an input to the Earth's environment, *International Solar Cycle Studies (ISCS) Symposium, 23 - 28 June 2003, Tatransk Lomnica, Slovak Republic. Ed.: A. Wilson. ESA SP-535, Noordwijk: ESA Publications Division*, ISBN 92-9092-845-X, 2003, p. 275
25. J. Kropp, and H.-J. Schellnhuber, In Extremis: Trends, Correlations, and Extremes in Hydrology and Climate, *Springer-Verlag*, Berlin (2010)
26. S. Lennartz, and A. Bunde, Trend Evaluation in Records with Long-term Memory: Application to Global Warming, *Geophys. Res. Lett.* **36**, L16706, doi:10.1029/2009GL039516 (2009a)
27. S. Lennartz, S, and A. Bunde, Eliminating finite-size effects and detecting the amount of white noise in short records with long-term memory, *Phys. Rev. Lett. E* **79**, p. 066101 (2009b)
28. S. Lennartz, and A. Bunde, Distribution of natural trends in long-term correlated records: A scaling approach, *Phys. Rev. E* **84**, 021129 (2011)
29. V.N. Livina, Y. Ashkenazy, Z. Kizner, V. Strygin, A. Bunde, and S. Havlin, A stochastic model of river discharge fluctuations, *Physica A* **330**, p. 283 (2003)
30. V.N. Livina, S. Havlin, and A. Bunde, Memory in the Occurrence of Earthquakes, *Phys. Rev. Lett.* **95**, 208501 (2005)
31. M. Lockwood, R.G. Harrison, T. Woollings, and S.K. Solanki, Are cold winters in Europe associated with low solar activity?, *Environ. Res. Lett.* **5**, 024001, doi:10.1088/1748-9326/5/2/024001 (2010)
32. M. Lockwood, Solar influence on the Earth's climate, ISSI Workshop "Observing & Modelling Earth's Energy Flow", 11. Jan. 2011
33. C. Loehle, Climate change: detection and attribution of trends from long-term geological data, *Ecolog. Model.* **171**, 433-450, doi:10.1016/j.ecolmodel.2003.08.013 (2004)
34. H. Lüdecke, R. Link, and F.-K. Ewert, How natural is the recent Centennial Warming? An Analysis of 2249 Surface Temperature Records, *International Journal of Modern Physics C*, to be published in Oct. 2011.
35. Q.-B. Lu, Cosmic-ray-driven-electron-induced reactions of halogenated molecules adsorbed on ice surfaces: Implications for atmospheric ozone depletion, *Physics Reports*, doi:10.1016/j.physrep.2009.12.002 (2009)

36. J. Luterbacher, D. Dietrich, E. Xoplaki, M. Grosjean, and H. Wanner, European Seasonal and Annual Temperature Variability, Trends, and Extremes Since 1500, *Science* **303**, p. 1499 (2004)
37. F. Lux, M. Ausloos, Market fluctuations I: Scaling, multiscaling, and their possible origins, in "the science of disasters", *Springer-Verlag*, Berlin, p. 373, chapter 13 (2002)
38. A. Mangini, C. Spötl, and P. Verdes, Reconstruction of temperature in the Central Alps during the past 2000 years from ^{18}O stalagmite record, *Earth and Planetary Science Letters* **235**, p. 741 (2005)
39. A. Mangini, P. Verdes, C. Spötl, D. Scholz, N. Vollweiler, and B. Kromer, Persistent influence of the North Atlantic hydrography on central European winter temperature during the last 9000 years, *Geophys. Res. Lett.* **34**, L02704, doi: 10.1029/2006GL028600, 2007
40. R.N. Mantegna, H.E. Stanley, An Introduction to Econophysics: Correlations and Complexity in Finance, *Cambridge University Press*, Cambridge (2000)
41. A. Moberg, D.M. Sonechkin, K. Holmgren, N.M. Datsenko, and W. Karlen, Highly variable Northern Hemisphere temperatures reconstructed from low-and high-resolution proxydata, *Letters to Nature* **433**, (7026), p. 613 (2005)
42. R.A. Monetti, S. Havlin, and A. Bunde, Long term persistence in the sea surface temperature Fluctuations, *Physica A* **320**, p. 581 (2003)
43. NOAA (2010), <http://www.ncdc.noaa.gov/paleo/pubs/pcn/>
44. NOAA (2005), Solanki, S.K., et al. (2005), 11,000 Year Sunspot Number Reconstruction, IGBP PAGES/World Data Center for Paleoclimatology , Data Contribution Series #2005-015, NOAA/NGDC Paleoclimatology Program, Boulder CO, USA
45. T.N. Palmer, Predicting uncertainty in forecasts of weather and climate, *Rep. Prog. Phys.* **63**, p. 71 (2000)
46. J.D. Pelletier, and D. L. Turcotte, Self-affine time series: II. Applications and models, *Adv. Geophys.* **40**, p. 91 (1999)
47. D. Rybski, A. Bunde, S. Havlin and H. von Storch, Long-term persistence in climate and the detection problem, *Geophys. Res. Lett.* **33**, L06718, doi:10.1029/2005GL025591 (2006)
48. D. Rybski, A. Bunde, and H. von Storch, Long-term memory in 1000-year simulated temperature records, *J. Geophys. Res.* **113**, D02106, doi:10.1029/2007JD008568 (2008)
49. D. Rybski, and A. Bunde, On the detection of trends in long-term correlated records, *Physica A* **388**, p. 1687 (2009)
50. N. Scafetta, P. Grigolini, T. Imholt, J. Roberts, and B. West, Solar turbulence in Earth's global and regional temperature anomalies, *Phys. Rev. E* **69**, 026303 (2004)
51. N.J. Shaviv, J. Veizer, Celestial driver of Phanerozoic climate?, *GSA Today* **3**(7) (2003)
52. S.K. Solanki, I.G. Usoskin, B. Kromer, M. Schüssler and J. Beer, An unusually active Sun during recent decades compared to the previous 11,000 years, *Nature* **431**, 7012, p. 1084 (2004)
53. H. Svensmark, T. Bondo, and J. Svensmark, Cosmic ray decreases affect atmospheric aerosols and clouds, *Geophys. Res. Lett.* **36**, L15101, doi:10.1029/2009GL038429 (2009)
54. P. Talkner, and R.O. Weber, Power spectrum and detrended Fluctuation analysis: Application to daily temperatures, *Phys. Rev. E* **62**, 150 (2000)

55. R.O. Weber, and P. Talkner, Spectra and correlations of climate data from days to decades, *J. Geophys. Res.* **106** (D17), 20, 131-20, 144 (2001)
56. W. Weber, Strong Signature of the Active Sun in 100 Years of Terrestrial Insolation Data, *Annalen der Physik* **522**, no. 6, p. 372, DOI 10.1002/andp201000019 (2010)
57. <http://www.wetterzentrale.de>
58. K. Yamasaki, L. Muchnik, S. Havlin, A. Bunde, and H.E. Stanley, Scaling and memory in volatility return intervals in financial markets, *PNAS* **102**, no. 26, p. 9424 (2005)
59. E. Zorita, T.F. Stocker and H. von Storch, How unusual is the recent series of warm years?, *Geophys.Res.Lett.* **35**, L24706, doi:10.1029/2008GL036228 (2008)
60. F.J. Zwiers, The detection of climate change, in Anthropogenic Climate Change, p. 163, *Springer*, New York (1999)